

Optimization of a Novel Activation-Repolarization Metric to Identify Targets for Catheter Ablation

Fernando O. Campos¹, Michele Orini², Ben Hanson², Peter Taggart², Pier Lambiase^{2,3}, Bradley Porter^{1,4}, Christopher Aldo Rinaldi⁴, Jaswinder Gill^{1,4}, Martin J. Bishop¹

¹ King's College London, London, United Kingdom

² University College London, London, United Kingdom

³ St Bartholomew's Hospital, London, United Kingdom

⁴ Guys and St Thomas' NHS Trust, London, United Kingdom

Abstract

Identification of targets for catheter ablation of arrhythmias remains a significant challenge. We have recently developed a novel substrate mapping procedure, termed the Reentry Vulnerability Index (RVI), which incorporates both activation (AT) and repolarization (RT) times to identify ablation targets. Despite showing promise in a series of experiments, the approach requires further development to enable its incorporation into a clinical protocol. The goal of this study was to use computer simulations to optimize the RVI procedure for its future usage within the clinic. A 2D sheet model was employed to investigate the behavior of the RVI algorithm under mapping catheters recordings resembling clinical conditions. Conduction block following premature stimulation was induced and mapped in a cardiac tissue model including repolarization heterogeneity. RVI maps were computed based on the difference between RTs and ATs between successive pairs of electrodes within a given search radius. A color map was then constructed to highlight small RVI values which identify vulnerable sites for reentry. Within 2D sheet models we show that RVI maps computed on sparse recording sites randomly placed on the tissue surface were in good agreement with high resolution maps. Moreover, RVI maps computed on recording sites resembling a decapolar electrode placed linearly as well as on a fan-like arrangement also captured regions of small RVIs. The RVI algorithm performed well under a wide range of clinically-relevant mapping conditions. The RVI metric was capable of identifying pro-arrhythmic regions which may be used to guide ablation.

1. Introduction

Ventricular tachycardias (VTs) are associated with a high risk of sudden death in patients with cardiovascular

diseases [1]. These VTs are mostly based on re-entry resulting from a trigger and an arrhythmogenic substrate [2]. Catheter ablation therapy continues to be the only potential curative treatment for VTs. However, success rates are low as the prediction of re-entrant circuits remain a significant clinical challenge. Ablation therapies usually target VT exit sites or areas of slow conduction based on activation-mapping or detection of fractionated electrograms [3]. However, in both such mapping procedures, the repolarisation landscape, a key factor in the success of a re-entrant circuit, is neglected in both mapping procedures. Consequently, identification of critical exit sites is hampered increasing the risk of later VT recurrence.

Recently, our group developed a novel mapping procedure, termed the Reentry Vulnerability Index (RVI), which incorporates not only activation (AT) but also repolarization (RT) times to identify ablation targets [4]. The algorithm has been shown to reliably identify the region of re-entry in *in-silico* [5], *in-vitro* [4] and in clinical [4,6] experiments. However, many questions regarding the mapping algorithm need to be fully addressed to enable its incorporation into a clinical protocol in an efficient and robust way. In particular, the density and sparsity of recording sites are highly dependent on the mapping system and might affect the ability of the RVI metric to discriminate VT circuits. The goal of this study is to use computational models to investigate the behavior of the RVI on electrode grids resembling clinically-relevant mapping conditions.

2. Methods

2.1. Computational Model

Electrical activity was simulated within a 5x5 cm finite element mesh (see Fig. 1) discretized at 200 μm resolution (62,500 quadrilateral elements). Ionic membrane dynamics were described by the Mahajan-Shiferaw (MSH) rabbit

ventricular cell model [7]. Ionic parameters were adjusted to produce a region of prolonged action potential duration (APD) in the lower half of the tissue (Fig. 1B - blue trace). Specifically, the conductance of the rapid delayed rectifier potassium current was reduced to 30% and the conductance of the slow delayed rectifier potassium current was reduced to 20%. Bulk conductivity in the model was set to be isotropic with a value of 0.136 S/m ensuring a re-entrant circuit could fit inside the 2D sheet.

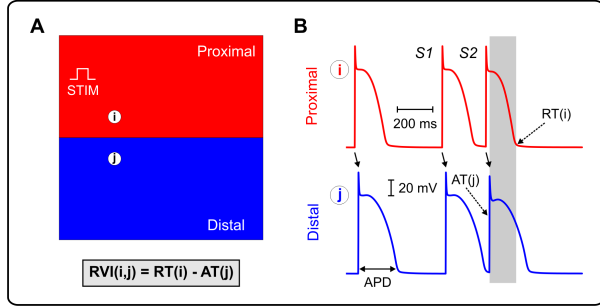


Figure 1. Schematic of the computational model. A) 2D sheet with proximal and distal regions. B) Action potentials following the S1S2 pacing protocol in cells from the proximal (red) and distal (blue) regions.

2.2. Pacing Protocol

Electrical activity was initiated following a S1S2 pacing protocol. Three S1 beats at cycle length of 500 ms followed by a premature S2 with coupling interval of 240 ms were simulated. Pacing was applied from a point in the upper left quadrant as shown in Fig. 1A.

Electrophysiological activity was simulated within the models using the Cardiac Arrhythmia Research Package (CARP) [8] (<http://carp.meduni-graz.at>). Throughout, a monodomain representation of tissue electrical dynamics was used with ionic dynamics represented by the MSH model.

2.3. Data Analysis

ATs and RTs are derived for all recording sites as the times at which the transmembrane potential (V_m) crossed -20 mV (with positive gradient) and -70 mV with (negative gradient), respectively. Recording grids with different densities were assessed:

- High-density grid: each finite element node in the 2D sheet was considered as a recording electrode;
- Clusters of electrodes: 40 clusters of random points located on the surface of the tissue model were selected as recording electrodes;
- Decapolar catheter: 10 recording electrodes (2-8-2mm

spacing) placed linearly as well as on a fan-like arrangement.

2.4. RVI Calculation

The RVI metric, originally idealized by Coronel *et al.* [2], quantitatively assesses the likelihood of wavefront-waveback interactions around a re-entrant circuit. If prematurely stimulated, cardiac tissue with prolonged refractoriness can lead to conduction block forcing the wavefront to travel around the line of block. If the proximal tissue, from where the wavefront originated, has completely repolarized then a re-entrant circuit ensues. Therefore, for two neighboring recording electrodes i and j spanning the line of block, the time interval between the RT of the proximal electrode i and the AT of the distal recording side j determines whether re-entry occurs:

$$RVI(i, j) = RT(i) - AT(j) \quad (1)$$

In case of normal propagation, $RVI(i, j)$ comes close to the APD of the tissue in the proximal region (see Fig. 1B). If a premature beat fails to immediately propagate to the distal region (unidirectional block), but travels along the line of block and back to the proximal region, $RVI(i, j)$ becomes small and its magnitude will depend on the repolarization state of the proximal region. If the proximal tissue has not completely repolarized, $RVI(i, j)$ will be small but positive (bidirectional block). However, if it repolarizes earlier (decreasing RT at i), or if the premature wavefront travels slower in the distal region (increasing AT at j), it will re-enter and $RVI(i, j)$ will be negative. Further details about the RVI metric can be found in Coronel *et al.* [2].

Child *et al.* [4] proposed an algorithm to map the RVI metric globally to identify regions capable of sustaining VT. As described in their study, ATs and RTs of a premature S2 beat are derived for all recording sites. Then, for a given recording site i all other sites j that are activated later than site i (*i.e.* are downstream neighbors of i) and lie within a prescribed search radius (R) are found. The RVI for each recording site pair $RVI(i, j)$ as in Eq. 1 is calculated. Finally, all RVIs associated with i are assigned to the geometric midpoint k between the pair of points i and j . A disadvantage of this interpolation approach is that it creates additional points (k) that may not in the original recording grid. Instead, in this study, the final RVI value at i is taken as the mean of all $RVI_s(i, j)$ associated with node i . A color map is then constructed to highlight small or negative RVI values to reveal the regions most vulnerable to re-entry.

3. Results

The S1S2 protocol was used to induce block and subsequent re-entry in the 2D sheet model. Fig. 2 shows the spatial distribution of V_m at different time instants following S1 and S2 beats. The S1 wavefront successfully propagates from the proximal to the distal side. The premature S2 beat, on the other hand, blocks at the distal region but travels towards the rightmost part of the tissue along the line of block (Fig. 2B, $t = 1310$ ms). Conduction block occurs because of the lengthened APD assigned to cells in the distal region (see Fig. 1B). Around $t = 1340$ ms, distal tissue at the end of the line of block has repolarized by the time the S2 wavefront arrives allowing it to travel back to the proximal region ($t = 1370$ ms in Fig. 2B). At $t = 1430$ ms the proximal tissue next to the stimulus site repolarizes allowing the wavefront to re-enter.

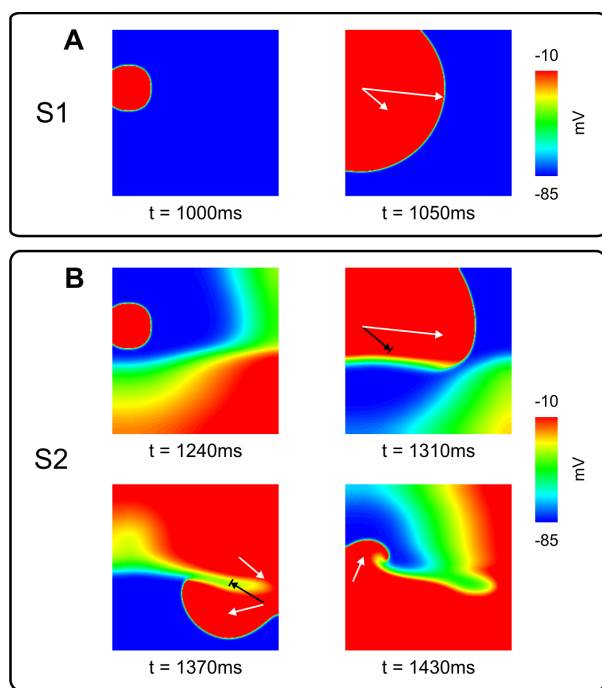


Figure 2. Spatial distribution of the transmembrane potential. A) Last S1 stimulus applied at $t = 1000$ ms. B) Re-entry induced by a S2 stimulus delivered at $t = 1240$ ms. White arrows: successful wavefront propagation; black arrows: conduction block.

Fig. 3A and Fig. 3B show ATs and RTs of the S2 beat in the 2D sheet, respectively. The line of unidirectional conduction block can be clearly seen from the AT sequence in Fig. 3A. The spatial RVI map constructed based on the ATs and RTs is shown in Fig. 3C. Note that the region of low RVIs distinctly coincides with the site of re-entry in Fig. 2 ($t = 1430$ ms).

In order to test whether the RVI can identify vulnera-

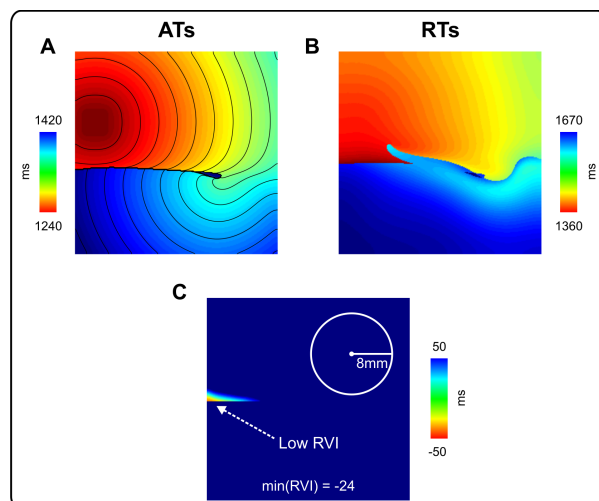


Figure 3. RVI calculation. A) ATs and B) RTs of the S2 beat. C) RVI map.

ble regions in clinically-relevant mapping conditions, RVI maps were computed on recording sites following different catheter arrangements. Fig. 4A presents the RVI map computed on clusters of recording electrodes randomly placed across the 2D sheet. Note that although there is a whole cluster next to the the critical region, only one electrode has a low RVI value (-24 ms). This is because the other electrodes have no downstream neighbors within the 8 mm search radius.

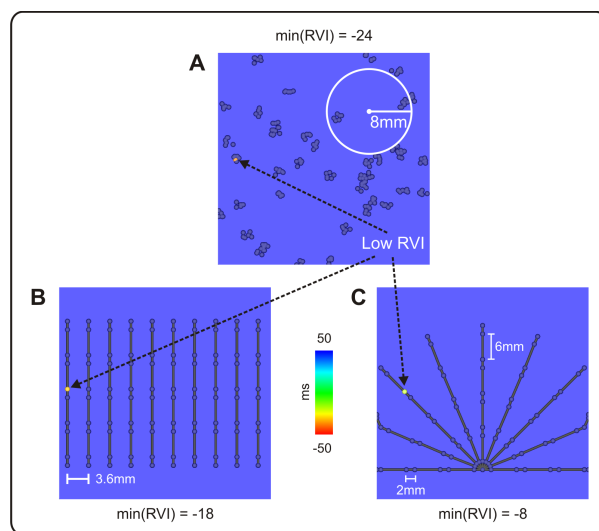


Figure 4. RVI maps constructed on different recording grids. A) Randomly distributed cluster of electrodes. B) Decapolar catheter placed linearly and C) on a fan-like arrangement.

In Fig. 4B-C, RVIs were computed on decapolar catheters (electrode spacing: 2-8-2mm) aligned vertically

as well as in a fan-like structure. In both cases, electrodes with small RVIs correspond to the region of low RVIs obtained on the high-density grid in Fig. 3C. The lowest RVI values in maps computed on the catheters placed linearly and on the fan-like arrangements are -18 ms and -8 ms, respectively. These are less negative than the lowest RVI obtained in the high-density case and in the clusters of recording electrodes, which produced a minimum value of -24 ms.

4. Discussion

In this study, we have used a 2D computational model to investigate the RVI algorithm in mapping conditions that mimic recording catheters used during catheter ablation procedures. Within a 2D sheet model with repolarization heterogeneity, we demonstrated that the RVI mapping can identify sites susceptible to reentry even in sparse recording grids similar to those available in the clinics.

The RVI algorithm has been shown to successfully identify VT exit sites in *in-silico* experiments with 2D tissue and whole ventricle models [4, 5]. However, RVI maps were computed based on ATs and RTs obtained on high-density grids or on structured grids with equally spaced recording points. In an ablation procedure, AT and RT sampling data varies due to the manual manipulation of the catheters. Here, we demonstrate that the RVI is capable of identifying sites prone to reentry even on sparse and unstructured recording grids resembling clinical conditions. As can be seen in Fig. 4, even one recording electrode is capable of highlighting the vulnerable area provided that there is at least one downstream neighbor within the search radius.

The use of a simple 2D cardiac tissue model facilitated the analysis of the influence of clinically-relevant mapping conditions on the RVI. However, the feasibility of the RVI mapping in more realistic cardiac models accounting for the irregularities in the ventricular geometry remains to be assessed.

In this study we have demonstrated with the aid of computer simulations, that the RVI algorithm was capable of identifying pro-arrhythmic regions under a wide range of clinically-relevant mapping conditions. Therefore, RVI may be of great value at guiding catheter ablation therapy of re-entrant arrhythmias.

Acknowledgements

This research was supported by the National Institute for Health Research (NIHR) Clinical Research Facility at Guy's and St. Thomas' National Health Service (NHS) Foundation Trust and NIHR Biomedical Research Centre based at Guy's and St. Thomas' NHS Foundation Trust and King's College London. The views expressed are

those of the authors and not necessarily those of the NHS, the NIHR or the Department of Health. FOC and MJB acknowledge the support of the British Heart Foundation through Project Grant PG/16/81/32441. MJB acknowledges the support of the UK Medical Research Council through a New Investigator Research Grant number MR/N011007/1.

References

- [1] Janse MJ, L. WA. Electrophysiological mechanisms of ventricular arrhythmias resulting from myocardial ischemia and infarction. *Physiol Rev* 1989;69(4):1049–169.
- [2] Coronel R, Wilms-Schopman FJ, Opthof T, Janse MJ. Dispersion of repolarization and arrhythmogenesis. *Heart Rhythm* 2009;6(4):537–43.
- [3] Wissner E, Stevenson WG, Kuck KH. Catheter ablation of ventricular tachycardia in ischaemic and non-ischaemic cardiomyopathy: where are we today? a clinical review. *Eur Heart J* 2012;33(12):1440–50.
- [4] Child N, Bishop MJ, Hanson B, Coronel R, Opthof T, Boukens BJ, Walton RD, Efimov IR, Bostock J, Hill Y, Rinaldi CA, Razavi R, J. G, Taggart P. An activation-repolarization time metric to predict localized regions of high susceptibility to reentry. *Heart Rhythm* 2015;12(7):1644–53.
- [5] Hill YR, Child N, Hanson B, Wallman M, Coronel R, Plank G, Rinaldi CA, Gill J, Smith NP, Taggart P, Bishop MJ. Investigating a novel activation-repolarisation time metric to predict localised vulnerability to reentry using computational modelling. *PLoS One* 2016;11(3):e0149342.
- [6] Martin CA, Orini M, Srinivasan NT, Bhar-Amato J, Honarbakhsh S, Chow AW, Lowe MD, Ben-Simon R, Elliott PM, Taggart P, Lambiase PD. Assessment of a conduction-repolarisation metric to predict arrhythmogenesis in right ventricular disorders. *Int J Cardiol* 2018;S0167-5273(18):32049–7.
- [7] Mahajan A, Shiferaw Y, Sato D, Baher A, Olcese R, Xie LH, Yang MJ, Chen PS, Restrepo JG, Karma A, Garfinkel A, Qu Z, Weiss JN. A rabbit ventricular action potential model replicating cardiac dynamics at rapid heart rates. *Biophys J* 2008;94(2):392–410.
- [8] Vigmond E, Hughes M, Plank G, Leon L. Computational tools for modeling electrical activity in cardiac tissue. *J Electrocardiol* 2003;36:69–74.

Address for correspondence:

Martin J. Bishop
School of Biomedical Engineering and Imaging Sciences, St Thomas' Hospital (4th Floor North Wing), SE1 7EH London, United Kingdom
martin.bishop@kcl.ac.uk